Carcinogenesis, 2020, Vol. 41, No. 2, 159–170

doi:10.1093/carcin/bgz132
Advance Access Publication July 12, 2019
Original Article

ORIGINAL ARTICLE

A trans-fatty acid-rich diet promotes liver tumorigenesis in HCV core gene transgenic mice

Xiao Hu[1,2], Xiaojing Wang[1,3], Fangping Jia[1], Naoki Tanaka[1,4,*], Takefumi Kimura[5], Takero Nakajima[1], Yoshiko Sato[6], Kyoji Moriya[7], Kazuhiko Koike[8], Frank J. Gonzalez[9], Jun Nakayama[6] and Toshifumi Aoyama[1]

[1]Department of Metabolic Regulation, Shinshu University School of Medicine, Matsumoto, Japan, [2]Department of Pathophysiology, Hebei Medical University, Shijiazhuang, People's Republic of China, [3]Department of Gastroenterology, Lishui Hospital, Zhejiang University School of Medicine, Lishui, Zhejiang, People's Republic of China, [4]Research Center for Social Systems, Shinshu University, Matsumoto, Japan [5]Department of Gastroenterology and [6]Department of Molecular Pathology, Shinshu University School of Medicine, Matsumoto, Japan, [7]Department of Infection Control and Prevention and [8]Department of Gastroenterology, The University of Tokyo, Tokyo, Japan and [9]Laboratory of Metabolism, National Cancer Institute, National Institutes of Health, Bethesda, MD, USA

*To whom correspondence should be addressed. Department of Metabolic Regulation, Shinshu University School of Medicine, Asahi 3-1-1, Matsumoto 390-8621, Japan. Tel: +81 263 37 2851;Email: naopi@shinshu-u.ac.jp

Abstract

Excess consumption of *trans*-fatty acid (TFA), an unsaturated fatty acid containing *trans* double bonds, is a major risk factor for cardiovascular disease and metabolic syndrome. However, little is known about the link between TFA and hepatocellular carcinoma (HCC) despite it being a frequent form of cancer in humans. In this study, the impact of excessive dietary TFA on hepatic tumorigenesis was assessed using hepatitis C virus (HCV) core gene transgenic mice that spontaneously developed HCC. Male transgenic mice were treated for 5 months with either a control diet or an isocaloric TFA-rich diet that replaced the majority of soybean oil with shortening. The prevalence of liver tumors was significantly higher in TFA-rich diet-fed transgenic mice compared with control diet-fed transgenic mice. The TFA-rich diet significantly increased the expression of pro-inflammatory cytokines, as well as oxidative and endoplasmic reticulum stress, and activated nuclear factor-kappa B (NF-κB) and nuclear factor erythroid 2-related factor 2 (NRF2), leading to high p62/sequestosome 1 (SQSTM1) expression. Furthermore, the TFA diet activated extracellular signal-regulated kinase (ERK) and stimulated the Wnt/β-catenin signaling pathway, synergistically upregulating cyclin D1 and c-Myc, driving cell proliferation. Excess TFA intake also promoted fibrogenesis and ductular reaction, presumably contributing to accelerated liver tumorigenesis. In conclusion, these results demonstrate that a TFA-rich diet promotes hepatic tumorigenesis, mainly due to persistent activation of NF-κB and NRF2-p62/SQSTM1 signaling, ERK and Wnt/β-catenin pathways and fibrogenesis. Therefore, HCV-infected patients should avoid a TFA-rich diet to prevent liver tumor development.

Introduction

Unsaturated fatty acids (FA), a major component of the human diet, generally contains one of two forms of double bonds: *cis* or *trans*. In *cis*-FA, the two carbon atoms forming double bonds bind two hydrogen atoms on the same side, leading to a curved conformation. In contrast, the two carbon atoms of the double bonds in *trans*-FA (TFA) bind two hydrogen atoms on diagonal sides of the carbon chain, resulting in a linear conformation. Despite equal numbers of atoms, these molecules exhibit distinctly different biological effects (1). TFA is naturally present at low levels in dairy products and animal meat but can be mass

Received: December 23, 2018; **Revised:** June 8, 2019; **Accepted:** July 11, 2019

Abbreviations

CCND1	cyclin D1
CK19	cytokeratin 19
DR	ductular reaction
ER	endoplasmic reticulum
ERK	extracellular signal-regulated kinase
FA	fatty acids
HCC	hepatocellular carcinoma
HCV	hepatitis C virus
HCVcpTg	HCV core gene transgenic
NF-κB	nuclear factor kappa B
NRF2	nuclear factor erythroid 2-related factor 2
PH	peroxisomal bifunctional protein
PPARα	peroxisome proliferator-activated receptor α
qPCR	quantitative polymerase chain reaction
SCD1	stearoyl-CoA desaturase 1
SEM	standard error of the mean
STAT3	signal transducer and activator of transcription 3
TFA	trans-fatty acid
TG	triglyceride
TLR	toll-like receptor

produced in the process of partial hydrogenation of vegetable oils, which are widely used in food manufacturing, commercial cooking and frying. Large amounts of artificial TFA are also included in shortening, margarine, cream cakes, fried fast food and some bakery products (2).

A recent prospective cohort study of 126 233 participants followed for as long as 32 years revealed that high TFA consumption was the strongest contributor to increased total mortality (3). Several reports have supported an association between excessive TFA intake and increased risks of coronary heart disease, obesity, metabolic syndrome, non-alcoholic fatty liver disease and other cardiovascular and metabolic diseases (4–6). Although the governments of North American and European countries have banned the use of TFA due to elevated disease risk, it is still widely used in food processing, and increasing in Asia (7). Increased TFA consumption is an emerging public health problem and clarifying the mechanism of its harmful effects is needed.

The influence of dietary TFA on the body has been debated mainly in the context of arteriosclerosis and metabolic syndrome. However, little is known about the impact of dietary TFA on carcinogenesis. Among several kinds of cancers, hepatocellular carcinoma (HCC) is reportedly the most significantly associated with obesity and metabolic syndrome (8), but whether excessive TFA consumption affects hepatocarcinogenesis remains unclear.

To address this issue, the impact of a TFA-rich diet was investigated using hepatitis C virus (HCV) core gene transgenic (HCVcpTg) mice. The mice exhibited hepatic steatosis, adenoma and HCC in a 'nodule-in-nodule' fashion in ~30% of males between 16 and 18 months of age and had been recognized as a mouse model of steatosis-derived HCC (9,10). Administration of a TFA-rich diet or an isocaloric control diet to the HCVcpTg mice for 5 months was carried out and liver phenotypes examined.

Methods

Mice and treatment

Male 12- to 13-month-old HCVcpTg mice on a C57BL/6 genetic background were used in this study (9–12). All mice were maintained in a pathogen-free environment under controlled conditions (25°C; 12 h light/dark cycle) with tap water and rodent laboratory purified control diet *ad libitum*, randomly divided into two groups and fed either a control diet (n = 17) or an isocaloric TFA-rich diet (n = 21) for 5 months. The control mice were also used in the previous study (13), and the diets were purchased from Research Diets (New Brunswick, NJ; D10012G and D14020301, respectively) and their detailed nutrient composition described previously (6). The TFA-rich diet was made by replacing 60 g of soybean oil in the purified diet (70 g total in 1000 g purified diet) with the same weight of Primex®, a commercial shortening containing large amounts of TFA, to produce identical calories per weight between the diets. The purpose of such replacement was to eliminate the effect of increased fat/calories by singularly adding TFA (6). A small amount of soybean oil was left for the prevention of essential FA deficiency (6). After treatment, the mice were anesthetized and killed by CO_2 asphyxiation at 6 h after food withdrawal for collection of blood and liver samples. Blood was centrifuged at 500*g* for 15 min twice to isolate serum. After the liver was removed, the liver surface was observed and the number and size of isolated tumors were measured. Subsequently, liver lobes were cut to 3–4 mm thickness using razors and the sections carefully evaluated to detect small tumors. If hepatic tumors were detected, they were dissected from the surrounding non-tumorous tissue and immediately frozen or fixed in 10% formalin in phosphate-buffered saline. Sera and non-tumorous liver tissues were immediately frozen as well and maintained at –80°C until evaluation. All animal experiments were conducted in accordance with animal study protocols outlined in the 'Guide for the Care and Use of Laboratory Animals' prepared by the National Academy of Sciences and were approved by Shinshu University School of Medicine before study commencement.

Biochemical analysis

Serum alanine aminotransferase, aspartate aminotransferase, alkaline phosphatase, triglyceride (TG), total cholesterol, total bile acid, non-esterified FA and glucose were measured with enzyme assay kits (Wako Pure Chemical Industries, Osaka, Japan) (13,14). Serum insulin concentrations were determined using the Mouse Insulin ELISA kit (TMB; AKRIN-011T; Shibayagi, Gunma, Japan). Liver lipids were extracted by the hexane:isopropanol method as described previously and quantified using enzymatic assay kits (Wako Pure Chemical Industries). Liver hydroxyproline contents were measured using the hydroxyproline assay kit (QuickZyme BioSciences, Leiden, the Netherlands) as described elsewhere (13).

Histological analysis

Small pieces of liver tissue were fixed in 10% formalin in phosphate-buffered saline and embedded in paraffin. Sections of 4 μm in thickness were stained with hematoxylin and eosin or Azan-Mallory staining using standard methods (15).

Expression of cytokeratin 19 (CK19) and β-catenin was analyzed by immunohistochemistry. Antigen retrieval was carried out by microwaving tissue sections in 10 mM Tris–HCl buffer (pH 8.0) containing 1 mM ethylenediaminetetraacetic acid for 30 min for anti-CK19 immunostaining, and in 10 mM citrate buffer (pH 6.0) for 30 min for anti-β-catenin immunostaining. The sections were incubated 1 h with an anti-CK19 antibody (TROMAIII, 1:100 dilution) and anti-β-catenin antibody (#9562, Cell Signaling, 1:200 dilution), respectively. The anti-CK19 antibody was obtained from the Developmental Studies Hybridoma Bank, created by The National Institute of Child Health and Human Development, National Institutes of Health, and maintained at The University of Iowa, Department of Biology (Iowa City, IA) (16). For secondary antibodies, Histofine Simple Stain Mouse MAX-PO (Rat) and Histofine Simple Stain MAX-PO (R), both purchased from Nichirei (Tokyo, Japan) were used. For immunodetection, peroxidase activity was visualized using diaminobenzidine–hydrogen peroxide solution. Specific staining was not detected in control experiments omitting the primary antibody. Pathological diagnosis was performed by J.N., a certified pathologist by the Japanese Society of Pathology, and N.T. in an independent and blinded manner.

Quantitative polymerase chain reaction analysis

Total liver RNA was extracted using an RNeasy Mini Kit (Qiagen, Tokyo, Japan) and reverse-transcribed to complementary DNA using oligo-dT and random primers with qScript cDNA SuperMix (Quanta BioSciences, MA). Levels of messenger RNA (mRNA) were measured by qPCR using an SYBR

qPCR kit (TOYOBO, Osaka, Japan) and Applied Biosystems StepOnePlus Real-Time PCR System (17,18). The primer pairs used are listed in Supplementary Table 1, available at *Carcinogenesis* Online. The mRNA levels were normalized to those of *18S* ribosomal RNA and expressed as fold changes relative to those of HCVcpTg mice fed a control diet.

Immunoblot analysis

Preparation of whole-liver homogenates was conducted as described previously, and liver nuclear fractions were isolated with NE-PER Nuclear and Cytoplasmic Extraction Reagents (Thermo Fisher Scientific, Rockford, IL). Protein concentrations were measured colorimetrically with a BCA Protein Assay Kit (Pierce, Rockford, IL) (19,20). Whole-liver homogenates (30–90 μg of protein in each lane) were subjected to sodium dodecyl sulfate–polyacrylamide gel electrophoresis at a polyacrylamide gel concentration of 7.5–10%. For analysis of the nuclear factor-kappa B (NF-κB) p65 component, peroxisome proliferator-activated receptor α (PPARα), β-catenin and glioma-associated oncogene homolog 1, nuclear fractions (40–45 μg of protein in each lane) were separated using 10% sodium dodecyl sulfate–polyacrylamide gel electrophoresis. After electrophoresis, the proteins were transferred to nitrocellulose or polyvinylidene fluoride membranes (Amersham Hybond-P, GE Healthcare, Little Chalfont, UK). The membranes were blocked for 1 h with 1–10% bovine serum albumin or 3–10% non-fat dry milk in Tris-buffered saline and incubated with the respective primary antibody overnight, followed next by incubation with alkaline phosphatase-conjugated secondary antibodies (#93785, Jackson ImmunoResearch Laboratories, West Grove, PA, 1:1000 dilution) and treatment with 1-step nitro blue tetrazolium chloride/5-bromo-4-chloro-3-indolyl-phosphate substrate (Pierce, Rockford, IL) (19,20), or horseradish peroxidase-conjugated secondary antibodies (#111-035-144, Jackson ImmunoResearch Laboratories, 1:4000 dilution) and treatment with Amersham ECL Prime Western Blotting Detection Reagents RPN2232 (GE Healthcare). The primary antibodies used in this study are shown in Supplementary Table 2, available at *Carcinogenesis* Online. True band positions were determined by co-electrophoresing molecular weight standards (Bio-Rad, Hercules, CA), with β-actin or histone H1 used as a loading control. Immunoblotting was repeated twice for each protein, and band intensities were quantified using NIH Image J (National Institutes of Health, Bethesda, MD), normalized to those of loading controls and subsequently expressed as fold changes relative to HCVcpTg mice fed a control diet.

Statistical analysis

Results are expressed as the mean ± standard error of the mean (SEM). The two-tailed Student's *t*-test and chi-squared test were conducted for quantitative and qualitative data, respectively, using SPSS statistics, version 22 (IBM, Armonk, NY). A P value < 0.05 was considered statistically significant.

Results

A TFA-rich diet enhances liver tumorigenesis in HCVcpTg mice

After treatment with a TFA-rich diet for 5 months, 100% of HCVcpTg mice exhibited liver tumors. The prevalence of tumors and isolated tumors with > 3 mm in diameter was significantly higher in TFA-rich diet-fed mice compared with control diet-fed mice (Figure 1A). The number of isolated tumors and maximal tumor size per mouse was also slightly greater in TFA-rich diet-fed mice (Figure 1A) but did not reach statistical significance. Although body weights were similar between the groups (P = 0.39), liver–body weight ratio, hepatic content of TG, total cholesterol and non-esterified FA and serum alanine aminotransferase levels were all significantly increased in the TFA diet-treated HCVcpTg mice compared with controls (Figure 1B and Supplementary Figure 2A, available at *Carcinogenesis* Online). Serum glucose levels were significantly elevated, whereas insulin levels were markedly decreased in TFA-rich diet-fed HCVcpTg mice (Supplementary Table 3, available at *Carcinogenesis* Online). Non-tumorous liver histology revealed more severe macrovesicular steatosis and inflammatory cell infiltration in TFA diet-treated HCVcpTg mice compared with the control ones (Figure 1C). These findings demonstrate that a TFA-rich diet enhances the development of hepatic steatosis, inflammation and tumors in HCVcpTg mice.

A TFA-rich diet alters hepatic lipid metabolism but does not activate PPARα in HCVcpTg mice

To examine the changes in hepatic lipid metabolism by a TFA-rich diet, the expression of the genes involved in FA and cholesterol metabolism was measured. *Cd36* mRNA encoding a transporter involved in FA uptake from the blood was significantly increased in the TFA-rich diet-fed HCVcpTg mice, but its protein levels were similar between the groups (Supplementary Figure 1A and B, available at *Carcinogenesis* Online). There were no remarkable differences in the mRNA and protein levels of FA-catabolizing enzymes, which included medium- and long-chain acyl-CoA dehydrogenases (*Acadm* and *Acadl*, encoding MCAD and LCAD, respectively) and acyl-CoA oxidase 1 (*Acox1*, encoding ACOX1), between the test groups (Supplementary Figure 1A and B, available at *Carcinogenesis* Online). The mRNA expression of the lipogenic enzymes acetyl-CoA carboxylase α (*Acaca*) and stearoyl-CoA desaturase 1 (*Scd1*, encoding SCD1) was increased by TFA-rich diet feeding (Supplementary Figure 1A, available at *Carcinogenesis* Online). No significant changes were detected in levels of mRNAs encoded by genes involved in FA transport and activation (*Fabp1* and *Acsl1*, encoding liver-type FA-binding protein [L-FABP] and acyl-CoA synthetase long-chain family member 1, respectively) or L-FABP protein levels (Supplementary Figure 1A and B, available at *Carcinogenesis* Online). Overall, upregulation of *Acaca* and *Scd1* mRNAs in the liver appeared to be associated with more severe FA/TG accumulation in high-TFA diet-fed HCVcpTg mice.

The mRNAs encoding hydroxymethylglutaryl-CoA synthase 1 and reductase (*Hmgcs1* and *Hmgcr*, respectively) tended to be increased by TFA diet treatment (Supplementary Figure 2B, available at *Carcinogenesis* Online). A significant upregulation was also detected in the mRNA levels encoding squalene epoxidase (*Sqle*), involved in cholesterol biosynthesis (Supplementary Figure 2B, available at *Carcinogenesis* Online). A high-TFA diet also increased the ATP-binding cassette subfamily A member 1 (*Abca1*), mRNA levels encoded by a liver X receptor target gene responsible for mobilizing cholesterol from the peripheral tissue and moderating cholesterol toxicity (Supplementary Figure 2B, available at *Carcinogenesis* Online). These changes were considered as a reason for the increased hepatic cholesterol content in high-TFA diet-fed HCVcpTg mice.

PPARα is a nuclear receptor mainly regulating lipid metabolism and its activation has been associated with hepatic tumorigenesis (21). The expression of proteins induced by PPARα activation, such as CD36, L-FABP, MCAD, LCAD, ACOX1 and peroxisomal bifunctional protein (PH), and nuclear PPARα levels were comparable between control diet- and TFA-rich diet-treated HCVcpTg mice (Supplementary Figure 1B and C, available at *Carcinogenesis* Online). These results indicate that a TFA-rich diet does not activate hepatic PPARα in this cohort.

A TFA-rich diet activates NF-κB by stimulating Toll-like receptors and inflammasomes in HCVcpTg mice

Liver tumorigenesis is driven by an altered hepatic microenvironment, such as inflammation, cellular stress and fibrosis. As elevated serum alanine aminotransferase and inflammatory cell infiltration were observed in TFA-rich diet-fed HCVcpTg mice,

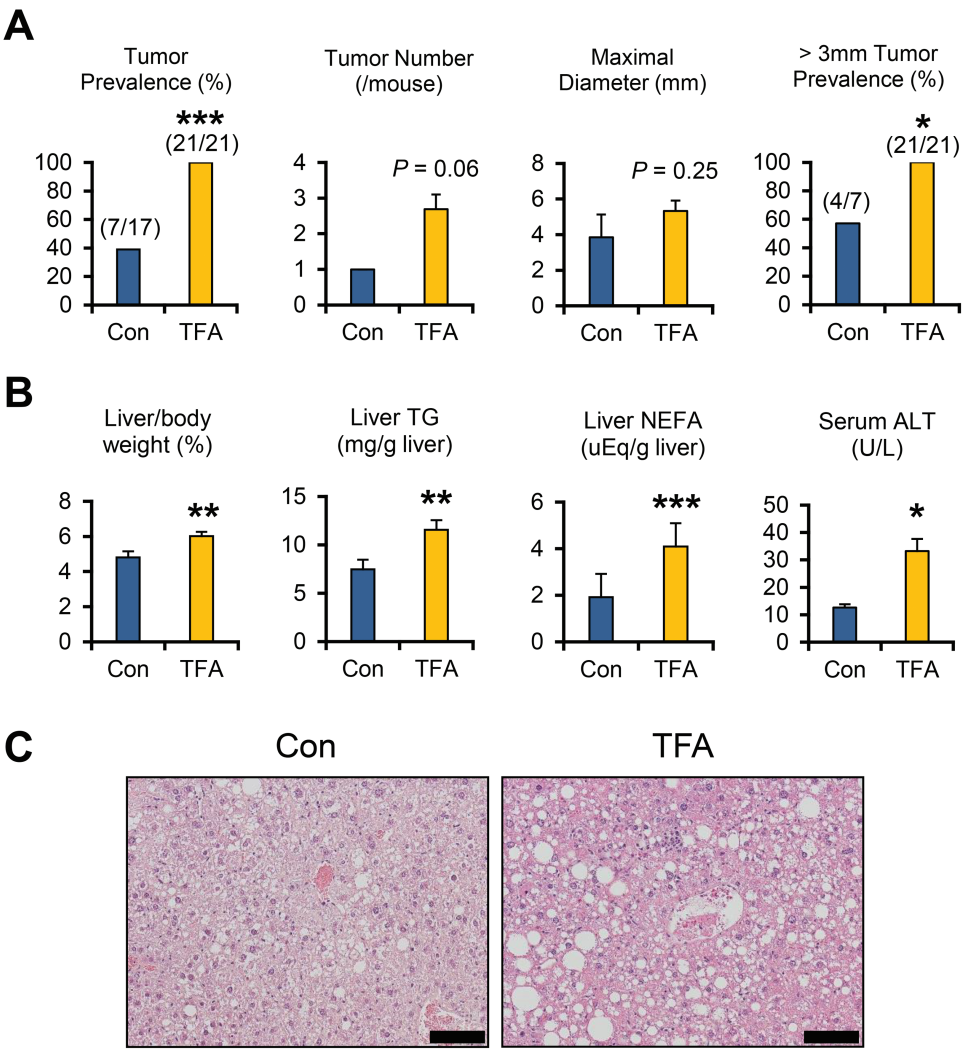

Figure 1. TFA-rich diet promotes the development of hepatic steatosis, inflammation and tumors in HCVcpTg mice. Male 12-13-month-old HCVcpTg mice on a C57BL/6 genetic background were treated for 5 months with a control diet (Con) or an isocaloric diet that replaced most FA with *trans*-FA (TFA). **(A)** Liver tumor prevalence rates, the number and maximal diameter of liver tumors in each mouse and prevalence rates of liver tumors > 3 mm in diameter. **(B)** Ratio of liver weight to body weight, hepatic content of triglyceride (TG) and non-esterified fatty acid (NEFA) and serum alanine aminotransferase (ALT) levels. **(C)** Photomicrographs of hematoxylin and eosin-stained liver sections. Bar = 100 μm. More severe macrovesicular steatosis and inflammatory cell infiltration were detected in TFA-rich diet-fed HCVcpTg mice. Data are expressed as mean ± SEM. *P < 0.05, **P < 0.01 and ***P < 0.001 between control diet-fed and TFA-rich diet-fed HCVcpTg mice.

the expression of key pro-inflammatory mediators was investigated. The mRNA levels of genes encoding pro-inflammatory cytokines released from M1 macrophages, specifically tumor necrosis factor α (*Tnf*), interleukin 1β (*Il1b*), C-C motif chemokine ligand 2 (*Ccl2*) and colony stimulating factor 1 (*Csf1*), were significantly increased in TFA-rich diet-fed HCVcpTg mice over controls (Figure 2A). The same tendency was observed for the *Arg1* mRNA encoding arginase 1, a hepatic M2 marker (Figure 2A). There were no remarkable differences in the mRNA levels of *Socs3* encoding suppressor of cytokine signaling 3, an indicator of another inflammatory signaling axis of interleukin 6-signal transducer and activator of transcription 3 (STAT3) (Figure 2A). The expression of these pro-inflammatory cytokines was induced by activation of NF-κB; immunoblot analysis using nuclear fractions revealed marked increases in nuclear p65 levels in TFA-rich diet-treated HCVcpTg mice over controls (Figure 2B), indicating significant activation of NF-κB in TFA-administered HCVcpTg mice.

Toll-like receptor (TLR) and inflammasome signaling are known to activate NF-κB (22). The genes associated with the TLR pathway (*Tlr2*, *Tlr4*, *Cd14* and *Myd88*) and inflammasomes (*Nlrp3*, *Asc*, *Panx1* and *Casp1*) were all simultaneously and significantly increased in HCVcpTg mice after TFA diet administration (Figure 2C), which were corroborated by increased protein levels in TLR2 and cleaved caspase 1 (Figure 2D). These results show that high TFA intake activates NF-κB via stimulation of TLRs and inflammasomes in HCVcpTg mouse livers.

A TFA-rich diet increases cellular stress and activates NRF2-p62/Sequestosome 1 signaling in HCVcpTg mice

Increased oxidative stress and endoplasmic reticulum (ER) stress cause DNA damage and contribute to liver tumorigenesis (23). The expression of mRNA encoding reactive oxygen species-generating enzymes, such as cytochrome b-245 beta chain (*Cybb*) and neutrophil cytosolic factor 1 (*Ncf1*), were similar between the test groups (Figure 3A). In contrast, the mRNA levels of genes encoding anti-oxidant enzymes including NAD(P)H quinone dehydrogenase 1 (NQO1, encoded by *Nqo1*),

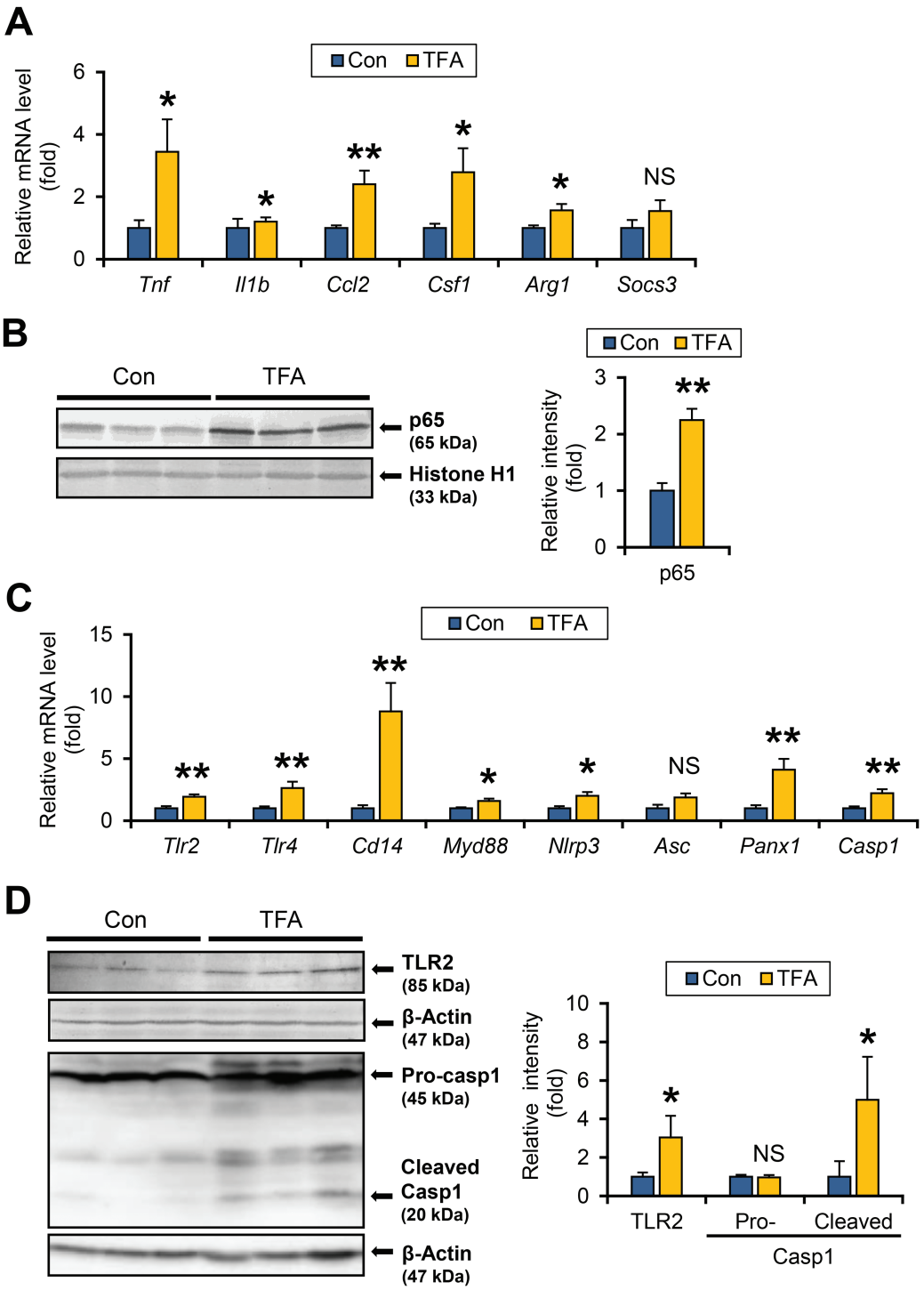

Figure 2. TFA-rich diet activates TLR/inflammasome and NF-κB signaling in HCVcpTg mice. **(A)** Hepatic mRNA levels of genes encoding M1 cytokines (*Tnf*, *Il1b*, *Ccl2* and *Csf1*), M2 cytokines (*Arg1*) and STAT3 signaling suppressor (*Socs3*) were quantified by qPCR, normalized to those of *18S* ribosomal RNA and expressed as values relative to HCVcpTg mice fed a control diet. **(B)** Immunoblot analysis of NF-κB p65. Liver nuclear fractions (40 μg of protein) were loaded into each well and the band of histone H1 was used as the respective loading control. Band intensities were measured densitometrically, normalized to those of histone H1 and expressed as values relative to HCVcpTg mice fed a control diet. Results were obtained from more than two independent immunoblot experiments and representative blots were shown. **(C)** Hepatic mRNA levels of genes related to TLRs (*Tlr2*, *Tlr4*, *Cd14* and *Myd88*) and inflammasomes (*Nlrp3*, *Asc*, *Panx1* and *Casp1*) were quantified by qPCR, normalized to those of *18S* ribosomal RNA and expressed as values relative to HCVcpTg mice fed a control diet. **(D)** Immunoblot analysis of TLR2 and caspase 1. Whole-liver homogenates (45–90 μg of protein) were loaded into each well and the band of β-actin was used as a loading control. The caspase 1 antibody detected pro-caspase 1 (45 kDa) and cleaved (activated) caspase 1 (20 kDa). Band intensities were measured densitometrically, normalized to those of β-actin and expressed as values relative to HCVcpTg mice fed a control diet. Results were obtained from two independent immunoblot experiments and representative blots were shown. Data are expressed as mean ± SEM. *P < 0.05, **P < 0.01 and ***P < 0.001 between control diet-fed and TFA-rich diet-fed HCVcpTg mice. Con, control diet-fed HCVcpTg mice; TFA, TFA-rich diet-fed HCVcpTg mice; NS, not significant.

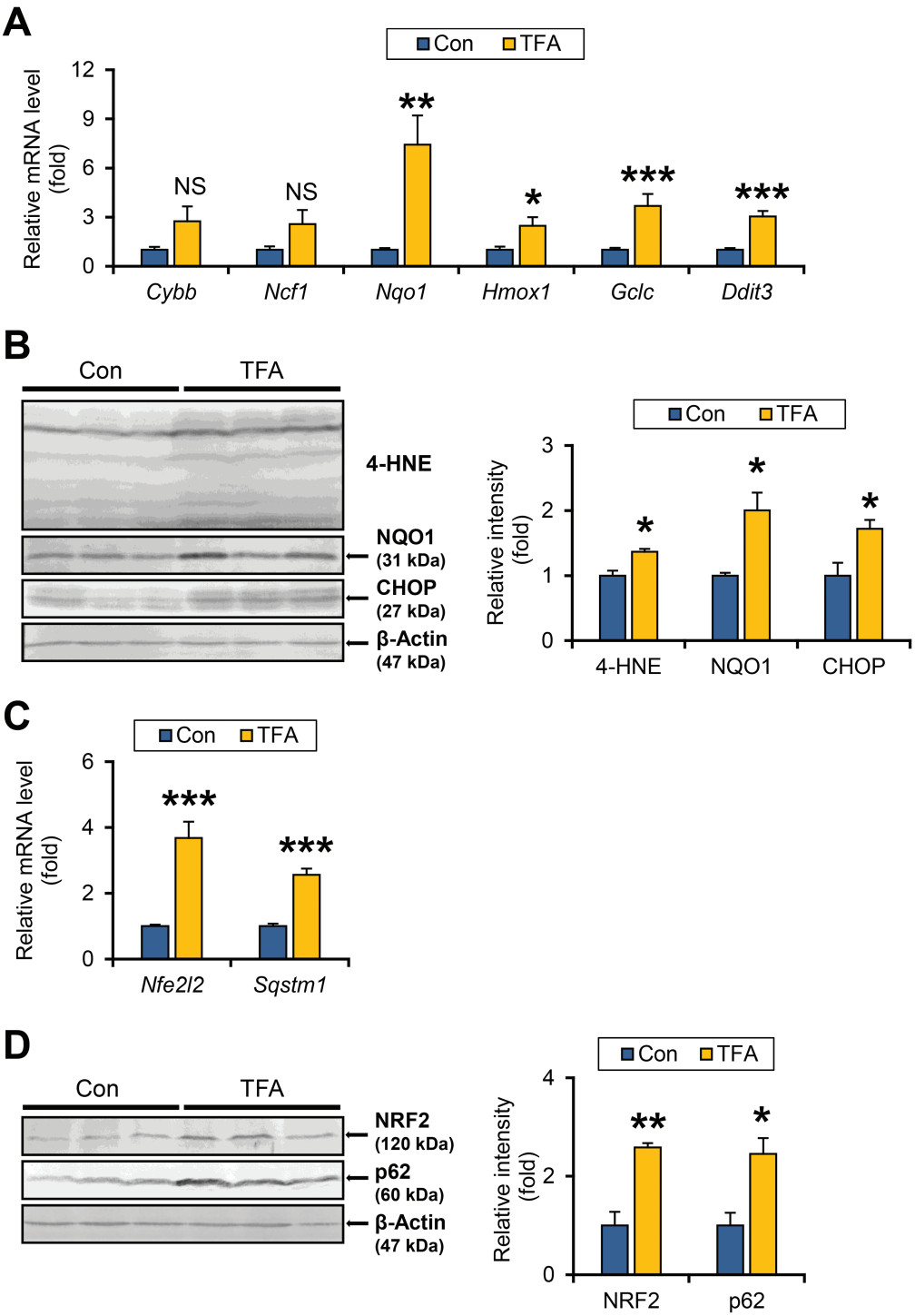

Figure 3. TFA-rich diet enhances oxidative/ER stress and activated NRF2-p62 signaling in HCVcpTg mice. **(A)** Hepatic mRNA levels of genes related to oxidative stress (*Cybb*, *Ncf1*, *Nqo1*, *Hmox1* and *Gclc*) and ER stress (*Ddit3*) were quantified by qPCR, normalized to those of *18S* ribosomal RNA and expressed as values relative to HCVcpTg mice fed a control diet. **(B)** Immunoblot analysis of 4-hydroxy-nonenal, NQO1 and C/EBP-homologous protein. Whole-liver homogenates (60–80 μg of protein) were loaded into each well and the band of β-actin was used as a loading control. Band intensities were measured densitometrically, normalized to those of β-actin and expressed as values relative to control diet-fed HCVcpTg mice. Results were obtained from two independent immunoblot experiments and representative blots were shown. **(C)** Hepatic mRNA levels of genes encoding NRF2 (*Nfe2l2*) and p62 (*Sqstm1*) were quantified by qPCR, normalized to those of *18S* ribosomal RNA and expressed as values relative to HCVcpTg mice fed a control diet. **(D)** Immunoblot analysis of NRF2 and p62. Whole-liver homogenates (60–80 μg of protein) were loaded into each well and the band of β-actin was used as a loading control. Band intensities were measured densitometrically, normalized to those of β-actin and expressed as values relative to HCVcpTg mice treated with a control diet. Results were obtained from two independent immunoblot experiments and representative blots were shown. Data are expressed as mean ± SEM. *$P < 0.05$, **$P < 0.01$ and ***$P < 0.001$ between control diet-fed and TFA-rich diet-fed HCVcpTg mice. Con, control diet-fed HCVcpTg mice; TFA, TFA-rich diet-fed HCVcpTg mice; NS, not significant.

heme oxygenase 1 (*Hmox1*) and glutamate–cysteine ligase catalytic subunit (*Gclc*) were significantly increased in TFA diet-fed HCVcpTg mice compared with controls (Figure 3A). Immunoblot analysis confirmed the elevated NQO1 expression and accumulation of 4-hydroxy-nonenal, a typical lipid peroxide, in the livers from mice on a TFA diet (Figure 3B). The mRNA levels of DNA damage-inducible transcript 3 protein (*Ddit3*) encoding C/EBP-homologous protein, a multifunctional transcription factor of ER stress, were also significantly increased in TFA-rich diet-treated HCVcpTg mice (Figure 3A and B). High TFA consumption thus appears to enhance hepatic oxidative stress and ER stress in HCVcpTg mice.

The autophagy adaptor protein p62/sequestosome 1 (hereafter, p62) is known to play a key role in HCC initiation and c-Myc induction. p62 is induced by the activation of NF-κB, ER stress and nuclear factor erythroid 2-related factor 2 (NRF2), a master regulator of redox state that protects cells against oxidative stress (24). The mRNA levels of *Nfe2l2* and *Sqstm1* encoding NRF2 and p62, respectively, were significantly elevated in HCVcpTg mice after treatment with a high-TFA diet (Figure 3C), which was confirmed at the protein levels (Figure 3D). NRF2 activation was also corroborated by upregulated NRF2 target genes, including *Nqo1*, *Hmox1* and *Gclc* (Figure 3A).

A TFA-rich diet drives fibrogenesis and ductular reaction in HCVcpTg mice

The impact of dietary TFA on the hepatic fibrosis-tumor axis was explored. Azan-Mallory staining revealed marked pericellular/perisinusoidal fibrosis in TFA-rich diet-fed HCVcpTg mice (Figure 4A). Enhanced liver fibrosis by a TFA diet administration was confirmed by increased hydroxyproline content (Figure 4B) and elevated mRNAs encoding transforming growth factor β1, α-smooth muscle actin (encoded by *Acta2*), collagen 1a1, connective tissue growth factor and osteopontin (encoded by *Spp1*) (Figure 4C). The increases in α-smooth muscle actin, connective tissue growth factor and osteopontin were corroborated by immunoblot analysis (Figure 4D).

Ductular reaction (DR) is pathologically defined as bile duct hyperplasia and is associated with liver fibrosis, liver damage and transdifferentiation and regeneration of hepatocytes (25). Indeed, a TFA-rich diet markedly enhanced proliferation of bile ducts, as revealed by anti-CK19 immunohistochemistry (Figure 4E). Expression of DR indicators and hepatic precursor markers, such as *Krt19*, *Afp*, *Epcam* and *Cd133* mRNAs, were higher in TFA-rich diet-treated HCVcpTg mice over controls (Figure 4F).

A TFA-rich diet promotes hepatocyte proliferation in HCVcpTg mice

As dysregulated cell cycle has been shown to play a critical role in the process of tumorigenesis (26), changes in the expression of cell cycle regulators were measured. The mRNA levels of cyclin D1 (CCND1), cyclin-dependent kinase 4 and proliferating cell nuclear antigen, encoded by *Ccnd1*, *Cdk4* and *Pcna*, respectively, were markedly increased in TFA-rich diet-fed HCVcpTg mice compared with control diet-fed mice (Figure 5A). The mRNA encoding c-Myc, a proto-oncogene strongly associated with hepatocarcinogenesis (27), also showed significant increases in TFA-rich diet-treated mice (Figure 5A). Upregulation of CCND1, proliferating cell nuclear antigen and c-Myc was confirmed by immunoblot analysis (Figure 5B). The mRNA expression of p53 was significantly increased in HCVcpTg mice after TFA treatment, whereas mRNA expression p21 remained unchanged (Figure 5A).

Hepatocyte proliferation and CCND1 expression are regulated by several intracellular signaling pathways, such as activation of STAT3 and mitogen-activated protein kinase (28). Although a TFA-rich diet did not have any impact on STAT3 phosphorylation, the TFA-rich diet promoted phosphorylation of extracellular signal-regulated kinase (ERK) 1/2 (Figure 5C). No significant increases were observed in phosphorylated c-jun N-terminal kinase, p38 and Akt by TFA-rich diet administration (data not shown).

A TFA-rich diet upregulates Wnt/β-catenin signaling in HCVcpTg mice

It is noteworthy that the TFA-rich diet increased *Myc* mRNA expression. Both c-Myc overexpression and Wnt/β-catenin signaling are closely associated with liver tumorigenesis (29,30). As *Myc* transcription was reportedly regulated not only by p62 but also by Wnt/β-catenin, Notch and hedgehog signaling (29,31), alterations to these pathways were evaluated. The mRNA levels of *Ctnnb1* and β-catenin target genes, hepatocyte nuclear factor 1α (*Tcf1*) and Axin 2 (*Axin2*) were significantly elevated in TFA diet-fed HCVcpTg mice (Figure 6A). In agreement with these findings, increased nuclear β-catenin content and β-catenin-positive hepatocytes were detected in HCVcpTg mice fed the TFA diet (Figure 6B and C, arrows). Immunohistochemistry revealed that β-catenin was also positive in proliferating bile ducts (Figure 6C, arrowheads). Stronger β-catenin expression and higher *Ctnnb1* and *Tcf1* mRNA levels in liver tumor tissue of TFA-rich diet-fed mice compared with non-tumor liver tissue (Figure 6D) revealed activation of Wnt/β-catenin signaling by TFA diet treatment, which is associated with liver tumorigenesis.

Similar mRNA levels of Notch target gene *p21* between the two diets (Figure 5A) indicated a lack of Notch signal activation. Although the mRNA levels of genes involved in hedgehog signaling, *Ptc1* and *Smo*, were increased and those of *Hhip*, a negative regulator of the hedgehog pathway were inversely reduced in HCVcpTg mice treated with TFA, nuclear glioma-associated oncogene homolog 1 levels were similar (Supplementary Figure 2C and D, available at *Carcinogenesis* Online). These results imply that a high TFA intake induces c-Myc expression, mainly due to upregulating p62 and Wnt/β-catenin signaling pathway, leading to promotion of hepatic tumorigenesis in HCVcpTg mice.

Discussion

Artificially produced during the process of partial hydrogenation of vegetable oils, TFA is more harmful to humans than its naturally existing unsaturated FA counterpart (4–6). However, insufficient attention has been given to the impact of TFA on HCC, one of the common forms of cancer in humans. This study revealed how dietary TFA disrupts two key drivers of liver tumorigenesis, hepatic microenvironment and intracellular signaling pathways, in HCVcpTg mice. A TFA-rich diet significantly enhanced oxidative and ER stress, activated NF-κB and NRF2-p62 axes, ERK and Wnt/β-catenin signaling, significantly upregulated c-Myc/CCND1 expression and enhanced cell division. Excess TFA intake promoted fibrogenesis and DR as well. These alterations synergistically and cooperatively drove the occurrence of liver tumors. To our knowledge, this is the first demonstration of a detailed *in vivo* mechanism explaining how high TFA consumption may promote liver tumorigenesis (Figure 6E).

The finding that TFA-rich diet did not activate hepatic PPARα prompted us to consider the presence of PPARα-independent mechanisms to enhance liver tumorigenesis. c-Myc expression promotes the transition from the G0/G1 to the S phase of the

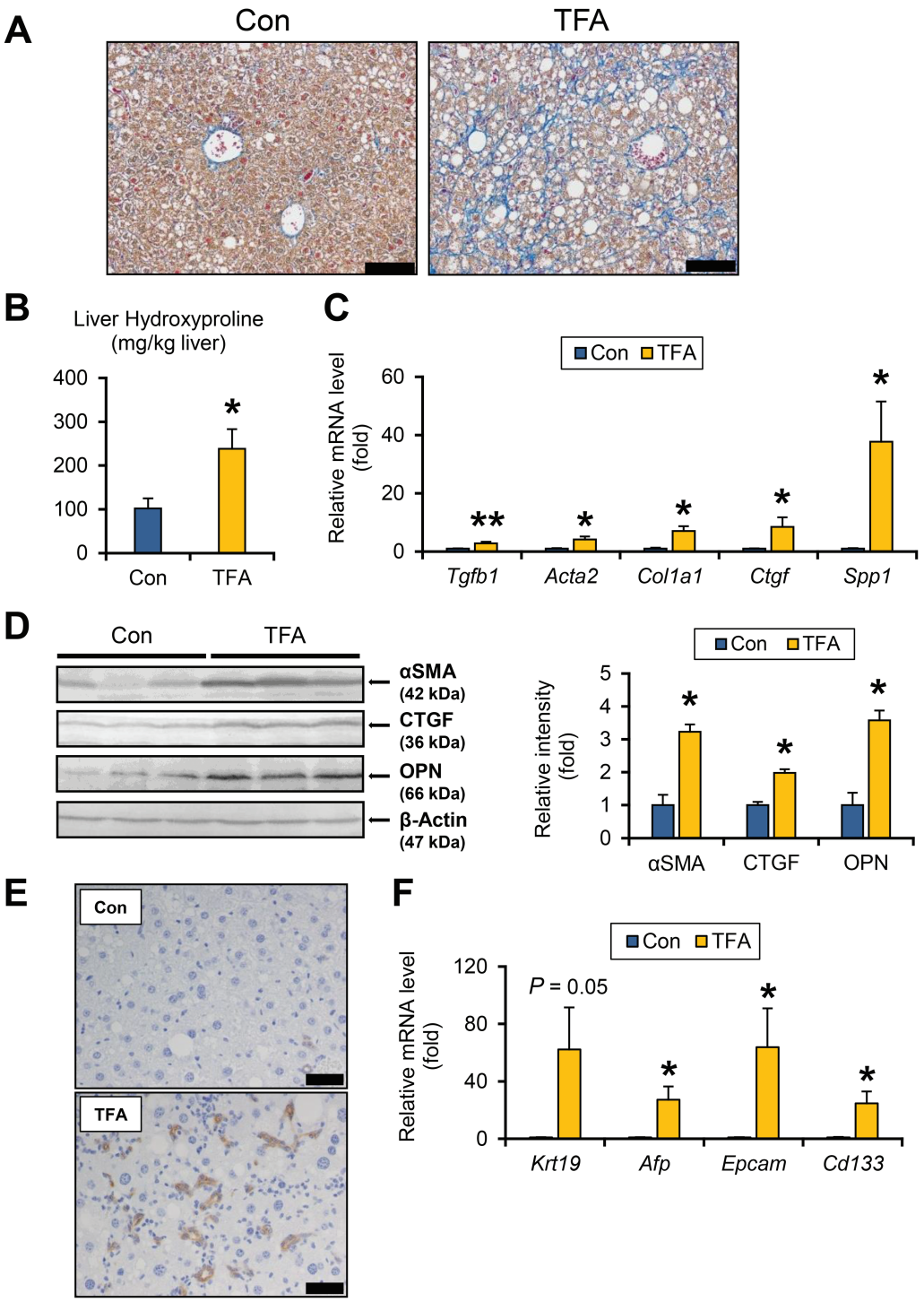

Figure 4. TFA-rich diet drives fibrogenesis and DR in HCVcpTg mice. **(A)** Representative photomicrographs of liver section stained with Azan-Mallory method. Bar = 100 μm. **(B)** Hepatic hydroxyproline contents. **(C)** Hepatic mRNA levels of genes related to fibrogenesis were quantified by qPCR, normalized to those of *18S* ribosomal RNA and expressed as values relative to HCVcpTg mice fed a control diet. **(D)** Immunoblot analysis of αSMA, connective tissue growth factor and osteopontin. Whole-liver homogenates (60–80 μg of protein) were loaded into each well and the band of β-actin was used as a loading control. Band intensities were measured densitometrically, normalized to those of β-actin and expressed as values relative to control diet-treated HCVcpTg mice. Results were obtained from two independent immunoblot experiments and representative blots were shown. **(E)** Immunohistochemical staining for CK19. Proliferation of CK19-positive biliary ducts was observed only in TFA-rich diet-treated HCVcpTg mice. Bar = 40 μm. **(F)** Hepatic mRNA levels of genes involved in DR and hepatocyte regeneration were quantified by qPCR, normalized to those of *18S* ribosomal RNA and expressed as values relative to control-diet fed HCVcpTg mice. Data are expressed as mean ± SEM. $^{*}P < 0.05$ and $^{**}P < 0.01$ between control diet-fed and TFA-rich diet-fed HCVcpTg mice. Con, control diet-fed HCVcpTg mice; TFA, TFA-rich diet-fed HCVcpTg mice.

cell cycle by regulating cyclin/cyclin-dependent kinase complexes (32). Hepatocyte-specific disruption of *Myc* produced a lower incidence of diethylnitrosamine-induced liver tumors, highlighting the crucial function of c-Myc in hepatocellular proliferation and liver tumorigenesis (27). Several signaling pathways are involved in the upregulation of c-Myc. Among them, the

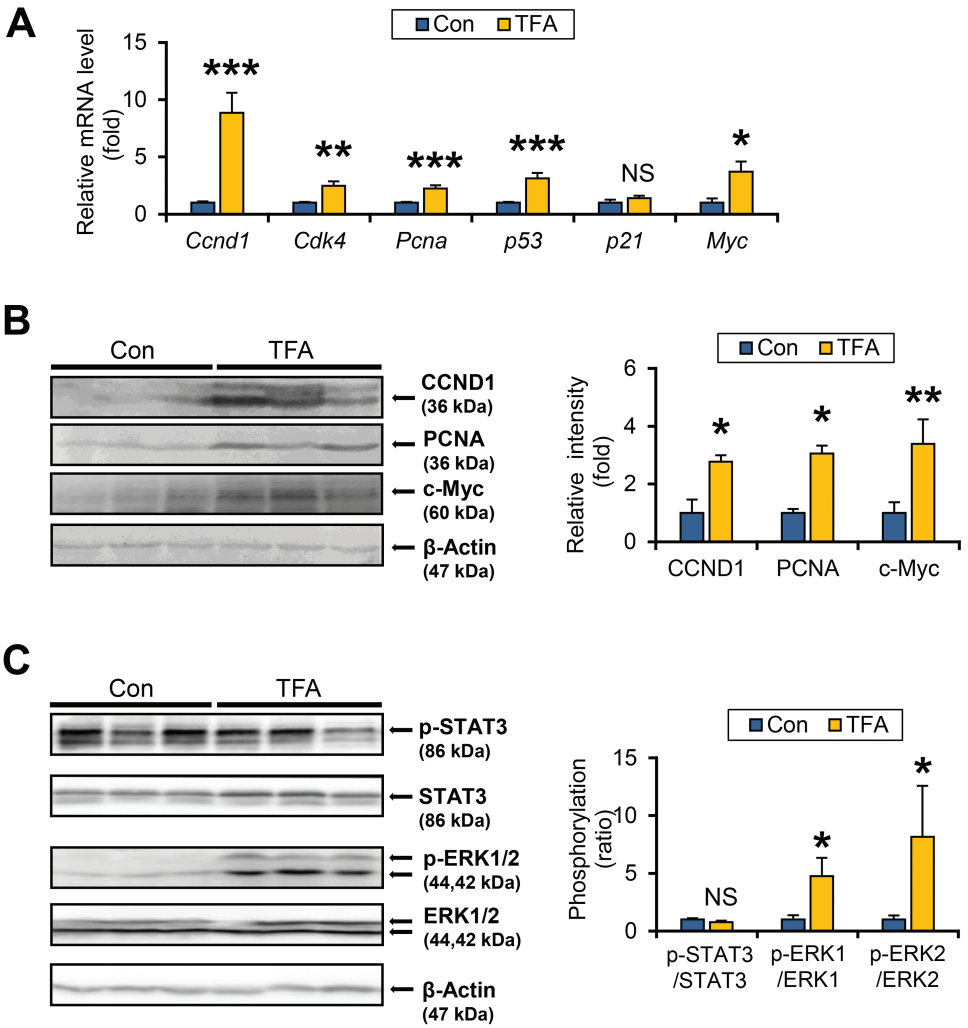

Figure 5. TFA-rich diet promotes ERK phosphorylation and hepatocyte proliferation in HCVcpTg mice. **(A)** Hepatic mRNA levels of cell cycle regulators were quantified by qPCR, normalized to those of *18S* ribosomal RNA and expressed as values relative to HCVcpTg mice fed a control diet. **(B)** Immunoblot analysis of CCND1, proliferating cell nuclear antigen and c-Myc. Whole-liver homogenates (60–80 μg of protein) were loaded into each well and the band of β-actin was used as a loading control. Band intensities were measured densitometrically, normalized to those of β-actin and expressed as values relative to HCVcpTg mice fed a control diet. Results were obtained from two independent immunoblot experiments and representative blots were shown. **(C)** Immunoblot analysis of STAT3 and ERK1/2. Whole-liver homogenates (45 μg of protein) were loaded into each well and the band of β-actin was used as a loading control. Band intensities were measured densitometrically, normalized to those of β-actin, calculated as phosphorylated/total ratio values and expressed as values relative to HCVcpTg mice fed a control diet. Results were obtained from two independent immunoblot experiments and representative blots were shown. Data are expressed as mean ± SEM. *P < 0.05, **P < 0.01 and ***P < 0.001 between control diet-fed and TFA-rich diet-fed HCVcpTg mice. Con, control diet-fed HCVcpTg mice; TFA, TFA-rich diet-fed HCVcpTg mice; NS, not significant; p-, phosphorylated.

Wnt/β-catenin pathway regulates the transcriptional activity of c-Myc and CCND1 (29) and β-catenin and its downstream genes were increased in TFA-rich diet-fed mice compared with control mice. Furthermore, Wnt/β-catenin activation was detected in liver tumors of TFA diet-treated mice. Enhanced Wnt/β-catenin signaling in the liver thus represents one of the mechanisms of accelerated liver tumorigenesis caused by high dietary TFA intake. These findings were partially in agreement with previous observations that high-fat diet-induced hepatosteatosis provoked Wnt/β-catenin activation and attenuated hepatosteatosis by calorie restriction depressed Wnt/β-catenin expression (33). Further studies are needed to fully elucidate the mechanism by which dietary TFA induces hepatic Wnt/β-catenin activation. In addition, as β-catenin was positively stained in hepatocytes and cholangiocytes of proliferating bile ducts in non-tumorous tissue of TFA-rich diet-fed mice, it deserves further investigations to determine which liver cells exhibiting high β-catenin expression play an important role in accelerating liver tumorigenesis induced by a TFA-rich diet.

NF-κB is a major transcription factor regulating inflammatory signaling, apoptosis and cell proliferation and plays a key role in inflammation-related hepatocarcinogenesis (34,35). Co-transfection of c-Myc oncogene promoter/exon 1-CAT plasmids with classical NF-κB (p65 alone or p65/p50) subunits constructed in NIH 3T3 cells exhibited significant expression of the *Myc* promoter, indicating an ability of NF-κB to induce c-Myc expression (36). In this study, long-term TFA intake resulted in augmentation of oxidative/ER stress, stimulation of TLRs and inflammasomes, activation of NF-κB and induction of p62, and presumably liver tumorigenesis promotion. Although other kinds of FA can serve as stimulators or activators of TLRs and inflammasomes (37,38), whether TFA singularly has such properties could not be assessed. Further studies are needed to specify the effect of TFA on immune and inflammatory responses.

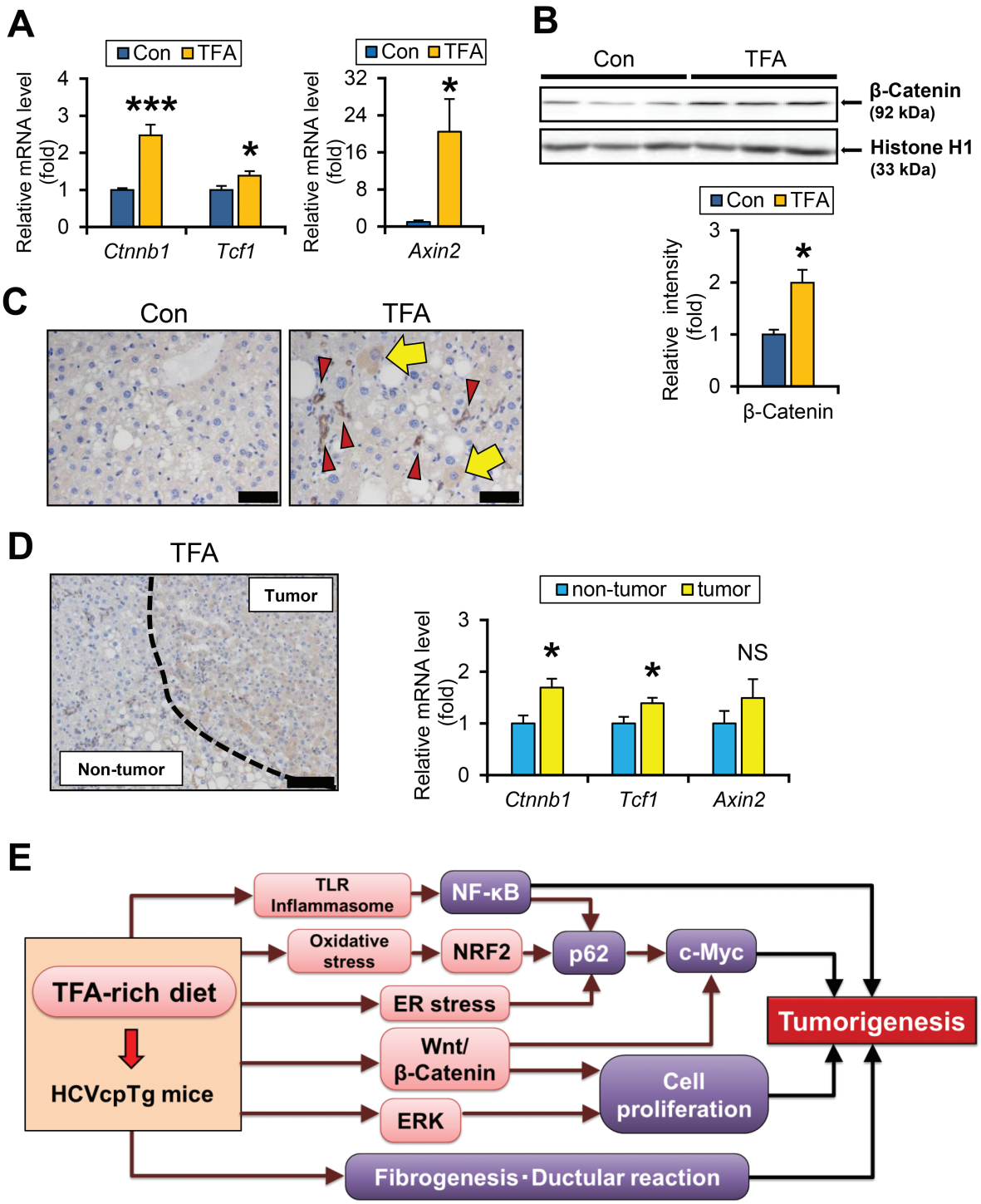

Figure 6. TFA-rich diet activates Wnt/β-catenin signaling in HCVcpTg mice. **(A)** Hepatic mRNA levels of genes associated with Wnt/β-catenin signaling were quantified by qPCR, normalized to those of *18S* ribosomal RNA and expressed as values relative to HCVcpTg mice fed a control diet. **(B)** Nuclear β-catenin levels. Liver nuclear fractions (45 μg of protein) were loaded into each well and the band of histone H1 was used as the respective loading control. Band intensities were measured densitometrically, normalized to those of histone H1 and expressed as values relative to HCVcpTg mice treated with a control diet. Results were obtained from two independent immunoblot experiments and representative blots were shown. **(C)** Immunohistochemical staining for β-catenin. In control HCVcpTg mice, β-catenin was weakly positive for cholangiocytes. In TFA-rich diet-fed mice, β-catenin was positively stained in some hepatocytes (arrows), as well as proliferating bile ducts (arrowheads). Bar = 40 μm. **(D**, left) Immunohistochemical staining for β-catenin in liver tumor of TFA-rich diet-fed HCVcpTg mice. β-catenin was intensely stained in tumor cells compared with the surrounding non-tumorous hepatocytes. Bar = 100 μm. **(D**, right) Comparison of β-catenin and its downstream signaling between tumorous and non-tumorous tissues in TFA-rich diet-fed HCVcpTg mice. The mRNA levels were quantified by qPCR, normalized to those of *18S* ribosomal RNA and expressed as values relative to non-tumorous tissue of TFA-rich diet-fed HCVcpTg mice. Data are expressed as mean ± SEM. *$P < 0.05$ and ***$P < 0.001$ between control diet-fed and TFA-rich diet-fed HCVcpTg mice. Con, control diet-fed HCVcpTg mice; TFA, TFA-rich diet-fed HCVcpTg mice; NS, not significant. **(E)** A proposed mechanism on how a TFA-rich diet promotes liver tumorigenesis in HCVcpTg mice.

Another intriguing finding was the remarkable upregulation of p62 by persistent consumption of TFA-rich diet. An autophagy adaptor and signaling protein, p62 is overexpressed in HCCs as well as in the surrounding pre-neoplastic liver tissue, and abnormal p62 accumulation occurs transcriptionally and post-transcriptionally. p62 transcription is induced by NF-κB and NRF2 (24). The strong p62 inducer NRF2 protects cells from oxidative stress and xenobiotic exposure by inducing genes encoding detoxification and oxidative stress-eliminating enzymes. However, NRF2 was also postulated to facilitate tumorigenesis by rescuing tumor-initiated cells from oxidative stress-induced death; NRF2 and antioxidant enzymes were overexpressed in carcinogen-induced aberrant hepatocyte foci in rats and various human cancer tissues. NRF2 promotes p62 accumulation and high amounts of p62 activate NRF2, forming a self-amplifying loop. Increased p62 also activates c-Myc signaling to promote cell proliferation. Moreover, the NRF2-p62 axis in HCC cells facilitates the glucuronate pathway and glutathione synthesis. This NRF2-dependent metabolic reprogramming accelerates cellular proliferation and drives tumorigenesis (39). Therefore, activation of the NRF2-p62 axis and ensuing p62 overexpression is probably a key contributor to liver tumorigenesis caused by the TFA-rich diet.

ERK signaling is one of the mitogen-activated protein kinase pathways and is closely associated with tumorigenesis via promoting cell proliferation and invasion. Inhibition of ERK phosphorylation suppresses CCND1 expression and leads to cell cycle arrest at G1 late phase, suggesting that ERK plays a crucial role in regulating CCND1 expression (40). A previous report revealed that hepatic steatosis increased ERK activity in *ob/ob* mice and high-fat diet-fed mice (41). Chemokines released from inflammatory cells and damaged hepatocytes are also considered as triggers of ERK activation (42). Activation of ERK by long-term TFA feeding also contributes to increased CCND1 expression, promoted hepatocyte proliferation and accelerated tumorigenesis in HCVcpTg mouse liver.

Most chronic liver diseases are accompanied by hepatic fibrosis (43–45). Although HCVcpTg mice showed no hepatic inflammation or fibrosis under regular conditions, a high TFA intake evoked inflammation and promoted liver fibrogenesis and DR. Pro-fibrogenic factors and extracellular matrices facilitate tumor cell proliferation and angiogenesis (46). DR is also linked with transdifferentiation and regeneration of hepatocytes (25), and increased expression of DR indicators and hepatic precursor markers, such as *Krt19*, *Afp*, *Epcam* and *Cd133*, were detected by the TFA-rich diet. These findings revealed in this study carry the important message that long-term TFA-rich diet consumption may cause liver fibrosis, DR and increases in hepatic progenitor cells, which may contribute to more liver tumors.

Nutrient metabolism is often altered in pre-cancerous and cancer cells. One common metabolic change is the overexpression of SCD1, an established molecular target in breast, colon, liver and other primary tumors that is associated with higher aggressiveness and poorer outcome in HCC (47). The upregulated SCD1 observed in the TFA-rich diet-fed HCVcpTg mice appeared to corroborate TFA's tumor-promoting properties.

This study is the first to focus on the impact of dietary TFA on HCV-mediated tumorigenesis. However, the small number of animals analyzed appeared to be a limitation of this study. In addition, it remains unclear whether the findings obtained in this study are specific to HCVcpTg mice or can apply to other models. Further studies are needed to clarify the impact of dietary TFA in other models of chronic liver disease and hepatocarcinogenesis to generalize from the findings uncovered in this investigation.

HCV eradication has long been regarded as the main aim for preventing HCV-related HCC. However, according to pandemic increases in obesity, metabolic syndrome and non-alcoholic fatty liver disease, metabolic aspects need also be considered in HCV-related hepatocarcinogenesis. The findings obtained in the current investigation indicate that restriction of TFA consumption may be useful to mitigate HCC development in HCV-infected patients. Clarifying the association between dietary fat composition and clinical outcome in HCV-infected patients would open new avenues regarding appropriate dietary management for HCC prevention.

Supplementary material

Supplementary data are available at *Carcinogenesis* online.

Funding

JSPS Grants in-Aid for Scientific Research (C) (KAKENHI Grant number 16K08616).

Acknowledgments

We thank Dr. Junpei Yamaguchi (Division of Surgical Oncology, Department of Surgery, Nagoya University Graduate School of Medicine) for providing anti-CK19 antibody and Mr. Trevor Ralph for his editorial assistance. We thank Research Center for Supports to Advanced Science (Shinshu University) for technical supports and animal care.

Conflict of Interest: The authors have declared that no conflict of interest exists.

References

1. Mensink, R.P. *et al.* (1993) Trans monounsaturated fatty acids in nutrition and their impact on serum lipoprotein levels in man. *Prog. Lipid Res.*, 32, 111–122.
2. Sommerfeld, M. (1983) Trans unsaturated fatty acids in natural products and processed foods. *Prog. Lipid Res.*, 22, 221–233.
3. Wang, D.D. *et al.* (2016) Association of specific dietary fats with total and cause-specific mortality. *JAMA Intern. Med.*, 176, 1134–1145.
4. Mozaffarian, D. *et al.* (2006) Trans fatty acids and cardiovascular disease. *N. Engl. J. Med.*, 354, 1601–1613.
5. Micha, R. *et al.* (2009) Trans fatty acids: effects on metabolic syndrome, heart disease and diabetes. *Nat. Rev. Endocrinol.*, 5, 335–344.
6. Hu, X. *et al.* (2017) PPARα protects against trans-fatty-acid-containing diet-induced steatohepatitis. *J. Nutr. Biochem.*, 39, 77–85.
7. Brouwer, I.A. *et al.* (2010) Effect of animal and industrial trans fatty acids on HDL and LDL cholesterol levels in humans–a quantitative review. *PLoS One*, 5, e9434.
8. Calle, E.E. *et al.* (2003) Overweight, obesity, and mortality from cancer in a prospectively studied cohort of U.S. adults. *N. Engl. J. Med.*, 348, 1625–1638.
9. Moriya, K. *et al.* (1998) The core protein of hepatitis C virus induces hepatocellular carcinoma in transgenic mice. *Nat. Med.*, 4, 1065–1067.
10. Moriya, K. *et al.* (1997) Hepatitis C virus core protein induces hepatic steatosis in transgenic mice. *J. Gen. Virol.*, 78 (Pt 7), 1527–1531.
11. Tanaka, N. *et al.* (2008) PPARalpha activation is essential for HCV core protein-induced hepatic steatosis and hepatocellular carcinoma in mice. *J. Clin. Invest.*, 118, 683–694.
12. Tanaka, N. *et al.* (2008) Hepatitis C virus core protein induces spontaneous and persistent activation of peroxisome proliferator-activated receptor alpha in transgenic mice: implications for HCV-associated hepatocarcinogenesis. *Int. J. Cancer*, 122, 124–131.
13. Wang, X., *et al.* (2019) A high-cholesterol diet promotes steatohepatitis and liver tumorigenesis in HCV core gene transgenic mice. *Arch. Toxicol.*, 93, 1713–1725.
14. Tanaka, N. *et al.* (2012) Disruption of phospholipid and bile acid homeostasis in mice with nonalcoholic steatohepatitis. *Hepatology*, 56, 118–129.

15. Tanaka, N. *et al.* (2014) Role of white adipose lipolysis in the development of NASH induced by methionine- and choline-deficient diet. *Biochim. Biophys. Acta*, 1841, 1596–1607.
16. Hayashi, Y. *et al.* (2018) Loss of trefoil factor 1 inhibits biliary regeneration but accelerates the hepatic differentiation of progenitor cells in mice. *Biochem. Biophys. Res. Commun.*, 506, 12–19.
17. Tanaka, N. *et al.* (2015) Adipocyte-specific disruption of fat-specific protein 27 causes hepatosteatosis and insulin resistance in high-fat diet-fed mice. *J. Biol. Chem.*, 290, 3092–3105.
18. Tanaka, N. *et al.* (2015) Role of fibroblast growth factor 21 in the early stage of NASH induced by methionine- and choline-deficient diet. *Biochim. Biophys. Acta*, 1852, 1242–1252.
19. Aoyama, T. *et al.* (1998) Altered constitutive expression of fatty acid-metabolizing enzymes in mice lacking the peroxisome proliferator-activated receptor alpha (PPARalpha). *J. Biol. Chem.*, 273, 5678–5684.
20. Tanaka, N. *et al.* (2017) Growth arrest and DNA damage-inducible 45α protects against nonalcoholic steatohepatitis induced by methionine- and choline-deficient diet. *Biochim. Biophys. Acta Mol. Basis Dis.*, 1863, 3170–3182.
21. Tanaka, N. *et al.* (2017) Targeting nuclear receptors for the treatment of fatty liver disease. *Pharmacol. Ther.*, 179, 142–157.
22. Pahl, H.L. (1999) Activators and target genes of Rel/NF-kappaB transcription factors. *Oncogene*, 18, 6853–6866.
23. Malhi, H. *et al.* (2011) Endoplasmic reticulum stress in liver disease. *J. Hepatol.*, 54, 795–809.
24. Umemura, A. *et al.* (2016) p62, Upregulated during preneoplasia, induces hepatocellular carcinogenesis by maintaining survival of stressed HCC-initiating cells. *Cancer Cell*, 29, 935–948.
25. Sato, K. *et al.* (2019) Ductular reaction in liver diseases: pathological mechanisms and translational significances. *Hepatology*, 69, 420–430.
26. Pascale, R.M. *et al.* (2002) Cell cycle deregulation in liver lesions of rats with and without genetic predisposition to hepatocarcinogenesis. *Hepatology*, 35, 1341–1350.
27. Qu, A. *et al.* (2014) Role of Myc in hepatocellular proliferation and hepatocarcinogenesis. *J. Hepatol.*, 60, 331–338.
28. Zhang, W. *et al.* (2002) MAPK signal pathways in the regulation of cell proliferation in mammalian cells. *Cell Res.*, 12, 9–18.
29. Yang, W. *et al.* (2008) Wnt/beta-catenin signaling contributes to activation of normal and tumorigenic liver progenitor cells. *Cancer Res.*, 68, 4287–4295.
30. Polakis, P. (2000) Wnt signaling and cancer. *Genes Dev*, 14, 1837–1851.
31. Patil, M.A. *et al.* (2006) Hedgehog signaling in human hepatocellular carcinoma. *Cancer Biol. Ther.*, 5, 111–117.
32. Dang, C.V. (1999) c-Myc target genes involved in cell growth, apoptosis, and metabolism. *Mol. Cell. Biol.*, 19, 1–11.
33. Debebe, A. *et al.* (2017) Wnt/β-catenin activation and macrophage induction during liver cancer development following steatosis. *Oncogene*, 36, 6020–6029.
34. Kumar, A. *et al.* (2004) Nuclear factor-kappaB: its role in health and disease. *J. Mol. Med. (Berl).*, 82, 434–448.
35. Pikarsky, E. *et al.* (2004) NF-kappaB functions as a tumour promoter in inflammation-associated cancer. *Nature*, 431, 461–466.
36. La Rosa, F.A. *et al.* (1994) Differential regulation of the c-myc oncogene promoter by the NF-kappa B rel family of transcription factors. *Mol. Cell. Biol.*, 14, 1039–1044.
37. Miura, K. *et al.* (2010) Role of toll-like receptors and their downstream molecules in the development of nonalcoholic fatty liver disease. *Gastroenterol. Res. Pract.*, 2010, 362847.
38. Henao-Mejia, J. *et al.* (2012) Inflammasome-mediated dysbiosis regulates progression of NAFLD and obesity. *Nature*, 482, 179–185.
39. DeNicola, G.M. *et al.* (2011) Oncogene-induced Nrf2 transcription promotes ROS detoxification and tumorigenesis. *Nature*, 475, 106–109.
40. Corona, G. *et al.* (2009) Hydroxytyrosol inhibits the proliferation of human colon adenocarcinoma cells through inhibition of ERK1/2 and cyclin D1. *Mol. Nutr. Food Res.*, 53, 897–903.
41. Jiao, P. *et al.* (2013) Hepatic ERK activity plays a role in energy metabolism. *Mol. Cell. Endocrinol.*, 375, 157–166.
42. McCubrey, J.A. *et al.* (2007) Roles of the Raf/MEK/ERK pathway in cell growth, malignant transformation and drug resistance. *Biochim. Biophys. Acta*, 1773, 1263–1284.
43. Sakurai, T. *et al.* (2013) Molecular link between liver fibrosis and hepatocellular carcinoma. *Liver Cancer*, 2, 365–366.
44. Kimura, T. *et al.* (2018) Mild drinking habit is a risk factor for hepatocarcinogenesis in non-alcoholic fatty liver disease with advanced fibrosis. *World J. Gastroenterol.*, 24, 1440–1450.
45. Kimura, T. *et al.* (2017) Clinicopathological characteristics of non-B non-C hepatocellular carcinoma without past hepatitis B virus infection. *Hepatol. Res.*, 47, 405–418.
46. Friedman, S.L. (2000) Molecular regulation of hepatic fibrosis, an integrated cellular response to tissue injury. *J. Biol. Chem.*, 275, 2247–2250.
47. Igal, R.A. (2011) Roles of stearoylCoA desaturase-1 in the regulation of cancer cell growth, survival and tumorigenesis. *Cancers (Basel).*, 3, 2462–2477.